Nanotechnology **20** (2009) 125302 (7pp) doi:10.1088/0957-4484/20/12/125302

Site-controlled lateral arrangements of InAs quantum dots grown on GaAs(001) patterned substrates by atomic force microscopy local oxidation nanolithography

J Martín-Sánchez, P Alonso-González, J Herranz, Y González and L González

Instituto de Microelectrónica de Madrid (CNM-CSIC), Isaac Newton 8 (PTM), 28760-Tres Cantos (Madrid), Spain

Received 17 December 2008, in final form 30 January 2009
Published 3 March 2009
Online at stacks.iop.org/Nano/20/125302

Abstract

In this work, we present a fabrication process that combines atomic force microscopy (AFM) local oxidation nanolithography and molecular beam epitaxy (MBE) growth techniques in order to control both the nucleation site and number of InAs quantum dots (QDs) inside different motifs printed on GaAs(001) substrates. We find that the presence of B-type slopes (As terminated) inside the pattern motifs is the main parameter for controlling the selectivity of the pattern for InAs growth. We demonstrate that either single InAs QDs or multiple InAs QDs in a lateral arrangement (LQDAs) can be obtained, with a precise control in their position and QD number, simply by varying the fabricated oxide length along the [110] direction.

(Some figures in this article are in colour only in the electronic version)

1. Introduction

Semiconductor quantum dots (QDs) have been intensely studied in recent years due to their quantum properties, which make them perfect candidates for the development of devices such as single-photon emitters for use in quantum information technologies [1, 2]. Additionally, it has been proved that the introduction of a controllable quantum coupling between two or more QDs in close proximity (quantum dot molecules, QDMs) is of great interest for further progress and new functionalities in the quantum computation field [3, 4]. The integration of such quantum structures (QDs and QDMs) in real and practical devices requires accurate technologies at the nanoscale that allow one to manage their position with high precision, as desired. Given that self-assembled InAs QDs and QDMs present random positions of nucleation, many efforts have been realized in order to control their site formation on patterned substrates [5–8] and to understand their formation process [9–12], although less work has been realized for a simultaneous control of both spatial localization and QD number in QDMs [13].

In this work, we combine atomic force microscopy (AFM) local oxidation nanolithography [14–16] and molecular beam epitaxy (MBE) growth techniques in order to obtain either site-controlled single InAs QDs or multiple InAs QDs in a lateral arrangement (LQDA) on GaAs(001) patterned substrates for their future validation as real lateral QDMs by optical characterization. For this purpose, we have fabricated site-controlled oxide dots and lines along [110], [1$\bar{1}$0] and [100] directions with an accurate control in their shape, size, and position by AFM local oxidation nanolithography on GaAs(001) substrates. After selective HF wet chemical etching of these oxides, nanometric motifs with the same size and shape as the negative AFM profiles of the initial oxides are obtained in a reproducible way. Therefore, round shaped nanoholes and elongated stripes with known size and shape are obtained from oxide dots and lines, respectively. The aim of this work is to use these motifs printed on the GaAs surface as preferential nucleation centres for InAs. Our results show that, depending on the oxide size, shape, and crystallographic orientation, single QDs or LQDAs with a precise control in the QD number can be obtained, either directly on GaAs(001)

patterned substrates or after growing a 7 nm thick GaAs buffer layer.

2. Experimental details

The epitaxial GaAs(001) substrates (ESs) used in this work were obtained by growing a 0.5 μm thick GaAs layer by MBE at a growth rate of 1 ML s^{-1}, substrate temperature T_S = 580 °C, and at a V/III flux ratio of 8. These epitaxial layers were grown on commercial epi-ready GaAs(001) substrates after the GaAs oxide was removed by a conventional thermal process: heating at T_S = 600 °C for 5 min under As_4 flux. Under the growth conditions used, flat surfaces at the atomic level, as measured by AFM, are obtained in a reproducible way.

Oxide dots and lines closely aligned along [110], [$\bar{1}$10], and [100] directions were fabricated on epitaxial substrates by AFM local oxidation nanolithography under ambient conditions at a relative humidity of about 30% using n-doped Nanosensor Si tips (K = 40 N m^{-1}). In our experimental set-up, the sample is set to ground and a negative bias voltage of −10 V is applied to the tip. In the case of oxide dot fabrication, while applying the bias voltage, the tip is maintained at a predefined position for 10 s. For oxide line fabrication of different submicron lengths, a scan writing speed of 0.035 μm s^{-1} is used.

The morphological characterization and fabrication of such oxides were realized in non-contact mode with a commercial Nanotec scanning probe microscopy (SPM) system provided with an optical set-up for spatial localization of patterned areas. When such oxides are selectively removed by a wet chemical etching with HF (49%) for 5 min, nanoholes that replicate the shape and dimensions of the negative oxide profile are obtained, in a systematic way, for both kinds of oxide structure. For subsequent epitaxial growth, the GaAs native oxide was removed in the MBE chamber by exposing the surface to an atomic hydrogen (H) flux using a Ta H_2 thermal cracker with a H_2 base pressure of 10^{-5} Torr for 30 min at low substrate temperature, T_S = 450 °C [17, 18]. Together with the H beam, As_4 was simultaneously supplied, at a beam equivalent pressure (BEP) of 5 × 10^{-7} Torr, to compensate arsenic losses from the surface. This low temperature process, instead of the conventional oxide thermal desorption process at T_S = 600 °C, is mandatory to preserve the tiny patterned motifs, as it is well known that Ga atom surface migration on GaAs(001) surfaces starts being significant for $T_S \geqslant$ 500 °C [19]. This means that it would be desirable to maintain the maximum temperature of the whole process as close as possible to 500 °C in order to avoid the smoothing of the nanoholes. At our low temperature process at T_S = 450 °C and after 5 min exposure to atomic H and As_4 beams, a clear c(4 × 4) As-rich surface reconstruction is observed on the reflection high energy electron diffraction (RHEED) pattern, indicating that the surface oxide has been removed. A long H + As_4 exposure and a distance of the QDs to the substrate interface as large as possible are crucial factors for obtaining an enhancement of the emission efficiency of InAs QD, as we have demonstrated in a previous work [20]. Accordingly, a H + As_4 exposure time of 30 min and a 7 nm thick GaAs buffer layer growth were used in this work. This GaAs buffer layer was grown by atomic layer MBE (ALMBE) [21] at T_S = 450 °C under an As_4 BEP of 2 × 10^{-6} Torr at a growth rate of 0.5 ML s^{-1}. This growth mode allows growing atomically flat GaAs epitaxial layers at low substrate temperatures without thickness limitation. We have explored the effect of growing this GaAs buffer layer on the selectivity of the pattern motifs for InAs growth. With this aim, 1.5 ML of InAs was deposited on patterned samples with and without a GaAs buffer layer. The InAs was deposited at 0.01 ML s^{-1}, T_S = 500 °C and an As_4 BEP of 5 × 10^{-7} Torr on a GaAs(001) surface showing a (2 × 4) surface reconstruction. Note that this InAs thickness is below the critical thickness for self-assembled QD formation (1.9 ML) on non-patterned substrates at the growth conditions used. In order to stabilize both the T_S at 500 °C and the As_4 pressure at 5 × 10^{-7} Torr for InAs deposition, a period of time of 5 min (annealing step) is introduced just before InAs deposition. After InAs growth, the samples were maintained at 500 °C for 2 min under As_4 flux. Then, they were cooled down and taken out of the system for AFM characterization.

We want to point out that the long time (30 min) of H+As_4 exposure, the GaAs buffer layer growth, the annealing step at 500 °C (5 min) substrate temperature, and As_4 pressure stabilization may produce a morphology (size and shape) change in the pattern motifs. For this reason, we have explored the evolution of the patterned motifs just before InAs deposition on patterned samples with and without a GaAs buffer layer. For this purpose, just after the thermal annealing step, the samples were cooled down and taken out of the system for AFM characterization.

Table 1. Average values of the difference between the dimensions of each nanohole and the initial motif, normalized to the dimensions of the initial motif. These values are obtained just before InAs deposition for the nanohole depth (d) and widths along the [110] (w[110]) and [$\bar{1}$10] (w[$\bar{1}$10]) directions. Results obtained for samples without and with a GaAs buffer layer growth are shown.

GaAs buffer thickness (nm)	W[110] (%)	W [$\bar{1}$10] (%)	d (%)
0	1 ± 1	−18 ± 2	20 ± 1
7	32 ± 2	−13 ± 2	−11 ± 1

3. Results and discussion

Figure 1 shows the evolution of the patterned motifs (nanoholes) with and without a GaAs buffer layer growth. The AFM images and profiles of the nanoholes were obtained after the HF wet chemical etching of the initial oxide motif (a), just before InAs deposition without GaAs buffer layer growth (b), and with the growth of a 7 nm thick GaAs buffer layer (c). The profiles obtained from each nanohole along the [110] and [$\bar{1}$10] directions are shown in figure 1(d). The results obtained for the nanohole evolution due to previously described processes before InAs deposition are summarized in table 1. There we show the average values, taken from eight nanoholes, of the difference between the dimensions of each resulting nanohole and the initial motif (nanohole after HF wet chemical etching), normalized to the dimensions of the initial

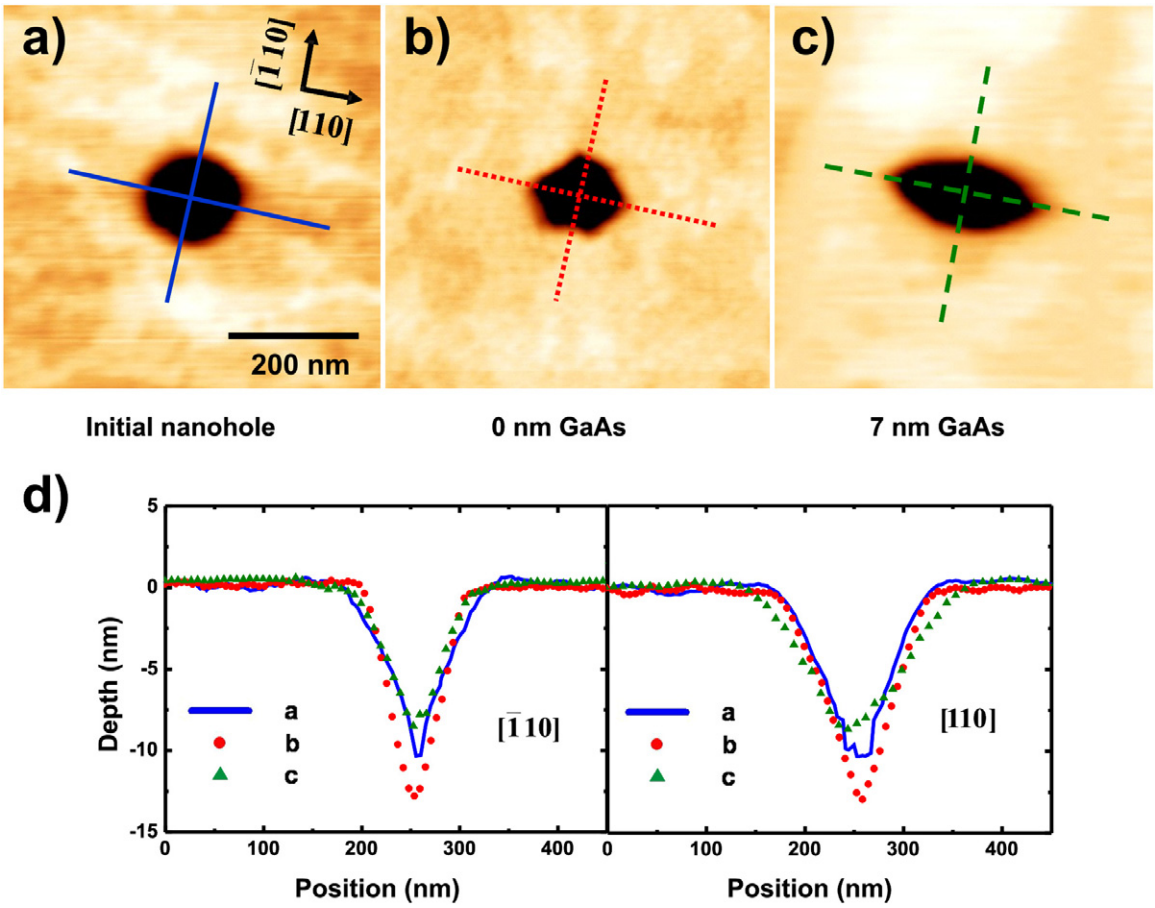

Figure 1. AFM images of the pattern motifs (nanoholes) obtained after HF (49%) wet chemical etching of the initial oxide (a), before InAs deposition without GaAs buffer layer growth (b), and with a 7 nm thick GaAs buffer layer growth (c). The profiles obtained from each nanohole along the [110] and [$\bar{1}$10] directions are shown in (d).

motif, for the nanohole depth (d) and width along the [110] ($w_{[110]}$) and [$\bar{1}$10] ($w_{[\bar{1}10]}$) directions. A positive (negative) value means an increase (decrease) of the specified nanohole dimension.

After HF wet chemical etching (figure 1(a)), the motif shows a clear round shape with a diameter of 160 nm and a depth of 10 nm. This round shape evolves to a hexagonal one (figure 1(b)) even without the growth of a GaAs buffer layer. These hexagonal holes show sides parallel to the [110] direction that correspond to the intersection of the B-type facets (As terminated) with the (001) surface plane. This experimental result on the nanohole evolution exhibits a similar qualitative behaviour to that previously reported by Heidemeyer *et al* [9] on motifs fabricated by e-beam lithography when GaAs buffer layers with increasing thickness were grown. In our case, a similar evolution is observed but without growing a GaAs buffer layer. When a 7 nm thick GaAs buffer layer is grown, although the hexagonal shape is blurred, a clear motif enlargement along the [110] direction occurs.

From the experimental values shown in table 1, we also observe that, for samples without a GaAs buffer layer, the resulting nanoholes are deeper than the initial ones. This behaviour has been previously reported for samples on which the oxide removal process has been carried out employing atomic H [5]. However, a decrease of the nanohole width along the [$\bar{1}$10] direction is common to the samples with and without GaAs growth. This fact could be related to the definition of B-type facets inside the motifs that, under certain growth conditions, incorporate Ga preferentially with respect to (001) surfaces [22, 23]. The Ga atoms incorporated at B-type walls would come from the MBE Ga source (only for samples with a GaAs buffer layer) and/or from the lateral movement of Ga surface atoms during the thermal annealing step. Nevertheless, the key point is that for both surface preparation processes (with or without GaAs buffer layer growth) the pattern motifs are preserved until the InAs deposition is performed.

In order to investigate the dependence of InAs nucleation process on the crystallographic orientation of the printed motifs, we have fabricated oxide lines (120 nm width, 500 nm length, and 8 nm height) along the [$\bar{1}$10], [010] and [110] crystallographic directions, as shown in figures 2(a1), (b) and (c), respectively. The results obtained after deposition of 1.5 ML of InAs on samples without a GaAs buffer layer show that a chain of three-dimensional (3D) InAs nuclei is formed in the stripes closely aligned along the [110] direction (see figure 2(f)). In contrast, no clear evidence of InAs nucleation is observed inside stripes aligned closely along the [$\bar{1}$10] and [010] directions (figures 2(d1), (e), (g) and (h)).

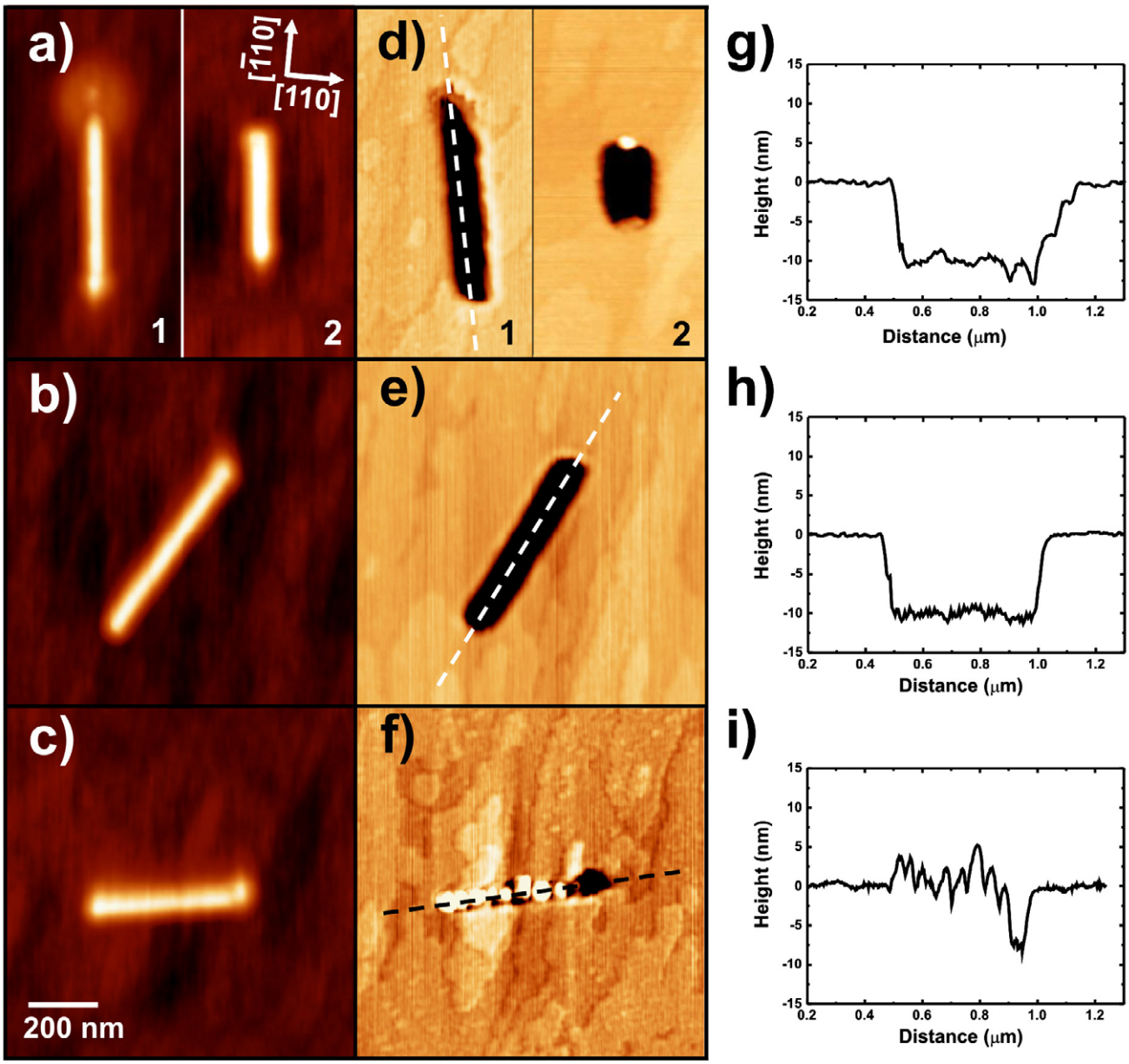

Figure 2. AFM images of initial oxide lines fabricated closely along the (a) [$\bar{1}$10], (b) [010], and (c) [110] directions. (d)–(f) show the results obtained on samples without a GaAs buffer layer, after the deposition of 1.5 ML of InAs at $T_S = 500\,^{\circ}$C. (g), (h), and (i) correspond to the profiles obtained on the AFM images of (d1), (e), and (f) respectively.

Only when the width of the pattern motifs aligned along the [$\bar{1}$10] direction is increased (from 120 to 160 nm, see figure 2(a2)), do isolated 3D nuclei appear leaning on their [110] sides (see figure 2(d2)). As we mentioned before, the motif sides along the [110] direction correspond to the intersection of the B-type facets (As terminated) with the (001) surface plane. Consequently, the extension of B-type facets is directly related with the length of [110] sides in the pattern motifs. These experimental results can be explained if the In atom incorporation, under the growth conditions used, is clearly higher on B-type facets (As terminated) inside the patterned stripes. Therefore, by increasing the B-slope areas inside the stripes, the incorporation rate of In atoms inside the pattern motifs increases, which finally determines the selectivity of the pattern for the InAs nucleation process.

In figure 3 we show AFM images of the initial oxide dots with lateral dimensions 160 nm × 160 nm (a), and the oxide lines fabricated closely along the [110] direction with lateral dimensions 160 nm × 230 nm (b), and 160 nm × 270 nm (c). The height of both the oxide dots and the lines is about 8 nm. The results obtained after deposition of 1.5 ML of InAs on these samples (after oxide etching) without a GaAs buffer layer growth demonstrate that, simply by varying the oxide size along the [110] direction from 160 to 270 nm, an isolated QD (figure 3(d)) or LQDA with two and three QDs (figures 3(e) and (f), respectively) can be obtained. These results are reproduced when a GaAs buffer layer is grown. We

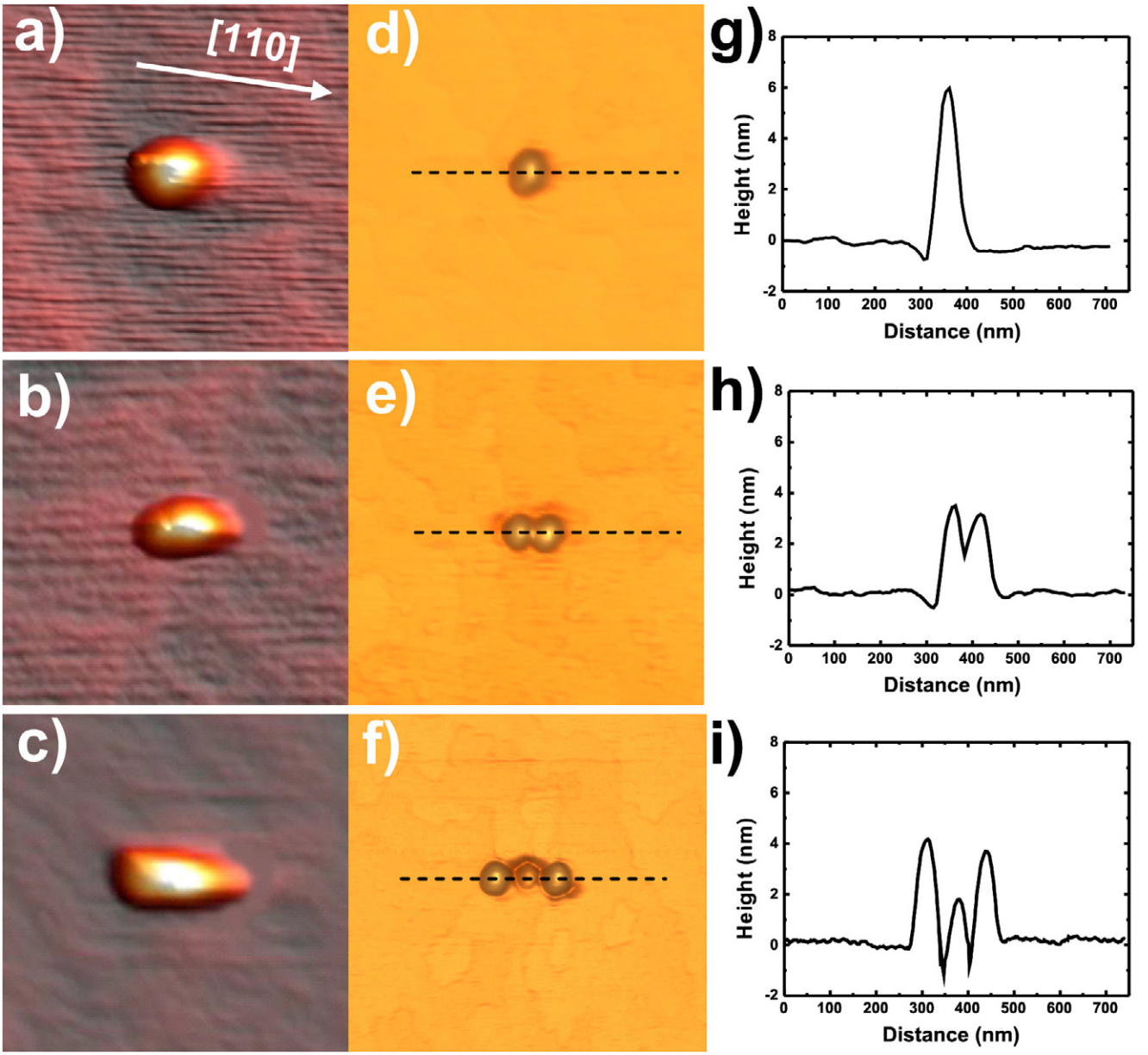

Figure 3. AFM images of the initial oxide dots with lateral dimensions 160 nm × 160 nm (a) and the oxide lines fabricated closely along the [110] direction with lateral dimensions 160 nm × 230 nm (b) and 160 nm × 270 nm (c). (d)–(f) show the results obtained after deposition of 1.5 ML of InAs on these pattern motifs on samples without a GaAs buffer layer. The profiles drawn along the lateral arrangements of InAs QDs obtained are depicted at the right-hand side, (g)–(i).

obtain an isolated single QD (figure 4(d)) from the initial round shaped oxide dot (figure 4(a)) and LQDA with two and three QDs (figures 4(e) and (f)) from initial oxide lines with lengths of 230 nm (figure 4(b)) and 270 nm (figure 4(c)) closely along the [110] direction. The average peak to peak interdot distance in the LQDA is 54 ± 3 nm, as measured on the AFM profiles shown in figures 3(h) and (i), and4(h) and (i). This interdot distance is short enough to ensure charge carrier interaction between adjacent QDs as previously reported [24]. Therefore, these results show that the number of QDs obtained inside patterned motifs can be controlled simply by varying the length of the initial oxide line along the [110] direction, with no limitations in QD number.

4. Conclusions

We have developed a fabrication process for obtaining site-controlled InAs single QDs or LQDAs by combining AFM local oxidation nanolithography and MBE growth techniques. We demonstrate that by controlling both the size and the shape of the initial oxide structures fabricated on epitaxial GaAs(001) substrates, as well as their crystallographic orientation, isolated QDs or LQDAs can be obtained with a great control in their positions, on GaAs(001) patterned substrates. We have found that the most relevant parameter in the fabrication process of LQDAs is the presence of B-type slopes inside the printed motifs, which can be increased by defining thin oxide lines (160 nm width) along the [110] direction.

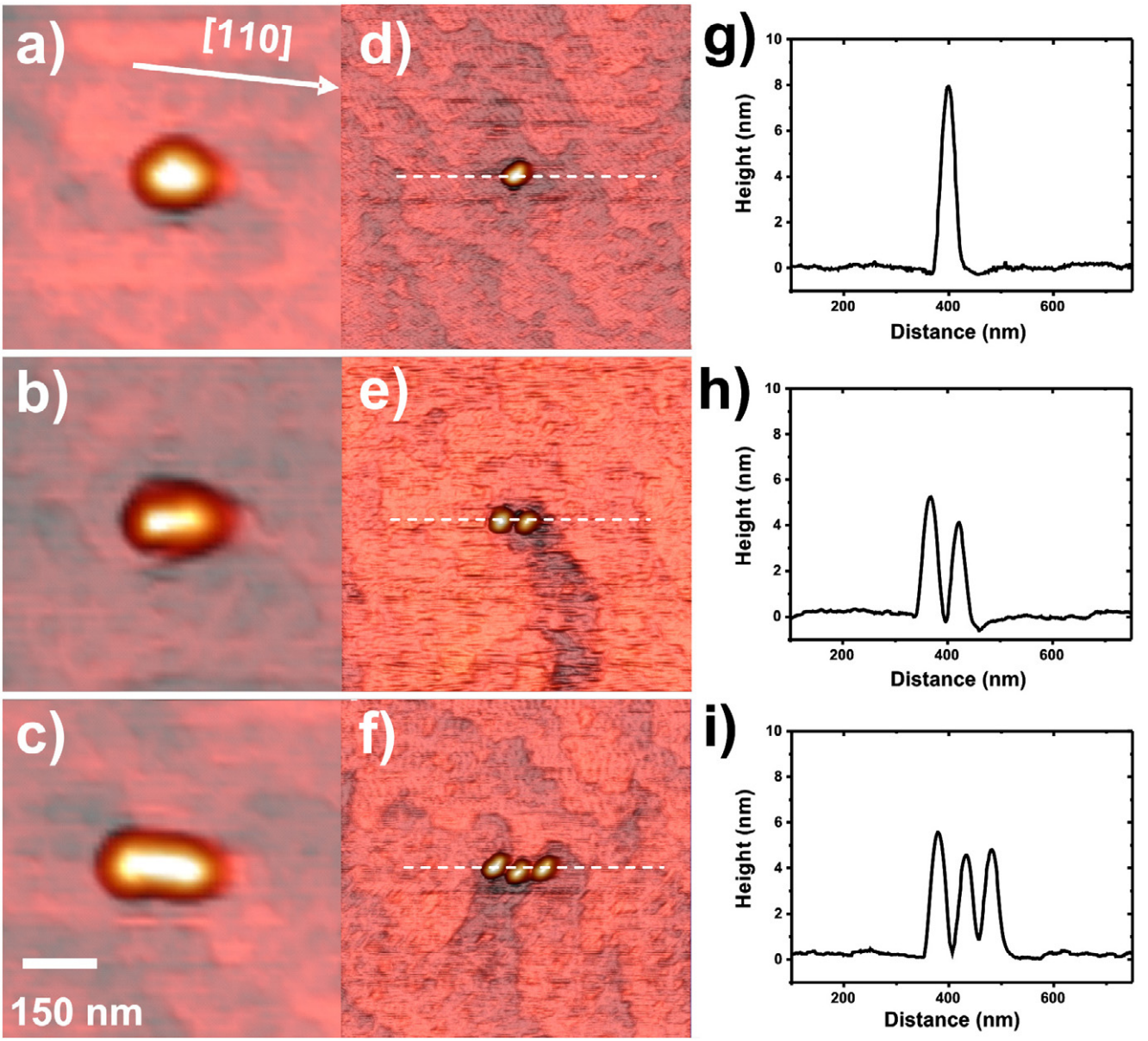

Figure 4. AFM images of the initial oxide dots with lateral dimensions 160 nm × 160 nm (a) and the oxide lines fabricated closely along the [110] direction with lateral dimensions 160 nm × 230 nm (b), and 160 nm × 270 nm (c). (d)–(f) show the results obtained after deposition of 1.5 ML of InAs on these pattern motifs on samples with a 7 nm thick GaAs buffer layer. The profiles drawn along the lateral arrangements of InAs QDs obtained are depicted at the right-hand side, (g)–(i).

The developed process is robust enough to permit the growth of a thin buffer layer without any loss in the control of the site formation of single QDs and lateral arrangements of different numbers of QDs, being so far fully compatible with the formation of high optical quality QDs and LQDAs.

Acknowledgments

This work was financed by Spanish MEC (TEC2008-06756-C03-01, NAN2004-09109-C04-01, Consolider-Ingenio 2010 CSD2006-00019), CAM (S 0505ESP 0200) and by the SANDIE Network of Excellence (Contract no. NMP4-CT-2004-500101 group TEP-0120). PAG, JH, and JMS thank the I3P programme.

References

[1] Santori C, Fattal D, Vuckovic J, Solomon G S and Yamamoto Y 2002 *Nature* **419** 594
[2] Stevenson R M, Young J, Atkinson P, Cooper K, Ritchie D A and Shields A J 2006 *Nature* **439** 179
[3] Taylor J M, Engel H A, Dür W, Yacoby A, Marcus C M, Zoller P and Lukin M D 2005 *Nat. Phys.* **1** 177
[4] Burkard G, Loss D and DiVicenzo D P 1999 *Phys. Rev.* B **59** 2070
[5] Atkinson P, Kiravittaya S, Benyoucef M, Rastelli A and Schmidt O G 2008 *Appl. Phys. Lett.* **93** 101908
[6] Schneider C, Straub M, Sünner T, Huggenberger A, Wiener D, Reitzenstein S, Kamp M, Höfling S and Forchel A 2008 *Appl. Phys. Lett.* **92** 183101
[7] Kiravittaya S, Songmuang R, Rastelli A, Heidemeyer H and Schmidt O G 2006 *Nanoscale Res. Lett.* **1** 1

[8] Pelucchi E, Watanabe S, Leifer K, Zhu Q, Dwir B, De Los Rios P and Kapon E 2007 *Nano Lett.* **7** 1282
[9] Heidemeyer H, Müller C and Schmidt O G 2004 *J. Cryst. Growth* **261** 444
[10] Lee J H, Wang Zh M, Strom N W, Mazur Yu I and Salamo G J 2006 *Appl. Phys. Lett.* **89** 202101
[11] Songmuang R, Kiravittaya S and Schmidt O G 2002 *Appl. Phys. Lett.* **82** 2892
[12] Siripitakchai N, Suraprapapich S, Thainoi S, Kanjanachuchai S and Panyakeow S 2007 *J. Cryst. Growth* **301/302** 812
[13] Wang L *et al* 2008 *New J. Phys.* **10** 045010
[14] García R, Calleja M and Heinrich R 1999 *J. Appl. Phys.* **86** 1898
[15] Okada Y, Amano S, Kawabe M and Harris J S 1998 *Appl. Phys. Lett.* **83** 7998
[16] Huang W P, Cheng H H, Jian S R, Chuu D S, Hsieh J Y, Lin C M and Chiang M S 2006 *Nanotechnology* **17** 3838
[17] Sugaya T and Kawabe M 1991 *Japan. J. Appl. Phys.* **30** L402
[18] Tomkiewicz P, Winkler A, Krzywiecki M, Chasse Th and Szuber J 2008 *Appl. Surf. Sci.* **254** 8035
[19] Kiravittaya S, Heidemeyer H and Schmidt O G 2004 *Physica* E **23** 253
[20] Martín-Sánchez J, González Y, Alonso-González P and González L 2008 *J. Cryst. Growth* **310** 4676
[21] Briones F, González L and Ruiz A 1989 *Appl. Phys.* A **49** 729
[22] Nishinaga T, Shen X Q and Kishimoto D 1996 *J. Cryst. Growth* **163** 60
[23] Kohmoto S, Nakamura H, Ishikawa T, Nishikawa S, Nishimura T and Asakawa K 2002 *Mater. Sci. Eng.* B **88** 292
[24] Li S S, Xia J B, Liu J L, Yang F H, Niu Z C, Freng S L and Zheng H Z 2001 *J. Appl. Phys.* **90** 6151